1973

Stopping power measurements of several solid composite materials for 1.9 to 3.3 MeV deuterons and 4.5 to 5.3 MeV alpha particles

Chester Louis Shepard
The University of Montana

STOPPING POWER MEASUREMENTS OF SEVERAL SOLID COMPOSITE MATERIALS FOR 1.9 TO 3.3 MeV DEUTERONS AND 4.5 TO 5.3 MeV ALPHA PARTICLES

by

Chester Shepard

B.A., University of Montana, 1970

Presented in partial fulfillment of the requirements for the degree of

Master of Arts

UNIVERSITY OF MONTANA

1973

Approved by:

Chairman, Board of Examiners

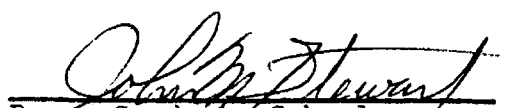

Dean, Graduate School

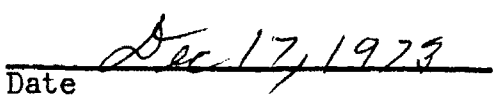

Date

ProQuest LLC.
789 East Eisenhower Parkway
P.O. Box 1346
Ann Arbor, MI 48106 - 1346

ACKNOWLEDGMENTS

The author would like to thank Ed Flynn, Judy Gursky, Stuart Orbesen, and Mal Wallis for their help in conducting the experimental work, and Dr. John Brolley for his kind hospitality while the author was at Los Alamos Scientific Laboratory. The author is particularly indebted to Dr. Leonard E. Porter for his help and encouragement in preparation of this thesis.

This work was supported in part by the U.S. Atomic Energy Commission. The author wishes to express his appreciation to Associated Western Universities for his appointment as a Thesis Parts Participant at the Los Alamos Scientific Laboratory.

TABLE OF CONTENTS

Chapter		Page
I.	INTRODUCTION	1
II.	THE DEUTERON EXPERIMENT	14
III.	THE ALPHA PARTICLE EXPERIMENT	23
IV.	FOIL PREPARATION	35
V.	ERROR ANALYSIS	39
VI.	RESULTS AND CONCLUSIONS	49
VII.	SUMMARY	59
LIST OF REFERENCES		62

LIST OF TABLES

Table		Page
1.	Deuteron Pulse Height Spectra Peak Locations	20
2.	Energy Losses	21
3.	Deuteron Stopping Powers	22
4.	Alpha Particle Pulse Height Spectra Peak Locations	28
5.	Energy Losses	32
6.	Alpha Particle Stopping Powers	33
7.	Foil Thickness Data	37
8.	Foil Composition	38
9.	Comparison of I_B with $\bar{I}$	52
10.	Mean Excitation Energies	53
11.	Comparison of I_B with $\bar{I}$ with Projectile z^3 Effect Included	57

LIST OF ILLUSTRATIONS

Figure		Page
1.	Deuteron Experimental Arrangement	15
2.	Energy Calibration - Deuteron Experiment	19
3.	Alpha Particle Experimental Arrangement	24
4.	Energy Calibration - Alpha Particle Experiment	31
5.	Typical Deuteron Spectrum	34
6.	Typical Alpha Particle Spectrum	34
7.	Background Subtraction	46
8.	Stopping Power Curves of Havar	61

CHAPTER I

INTRODUCTION

Due to both experimental and theoretical interests, the past years have seen many measurements of energy loss of charged particles in matter. In considering energy loss phenomena, charged particles can be classified as in one of two groups: electrons or heavy charged particles (e.g. protons, deuterons, and alpha particles). The difference in the behavior of electrons as compared to heavy charged particles is due to the fact that the electron rest mass is very small compared to the rest mass of heavy charged particles. As an example, in the velocity region where the most important interaction in energy loss phenomena is that between the incident charged particle and the electrons of the material, a heavy charged particle will lose only a small fraction of its total kinetic energy and will be deflected only slightly from its original path in a collision with an electron. An electron in a similar collision may lose a large amount of its kinetic energy and may be deflected by a large angle from its original path. All of the following discussion will be concerned with heavy charged particle interactions with matter.

The interaction of heavy charged particles with matter can be separated into three broad groups: interaction with the electrons of the atoms which the material comprises, interactions with the nuclei, and interactions with the atoms as a whole. Interactions with the atom as a whole occur exclusively at low incident particle energies. At higher

energies (greater than .5 MeV per nucleon) the incident particle interacts with the electrons and the nuclei separately. Interactions with the nuclei include nuclear reactions, nuclear scattering and Rutherford scattering.

If a large number of monoenergetic particles pass through a material of given thickness, they will have a distribution of energy after passage due to the statistical nature of energy loss associated with the above interactions. For a given thickness of material, not all particles will lose the same amount of energy in traversing that thickness. This phenomenon is known as energy straggling. Closely related to this is range straggling. For incident energies not extremely relativistic, an initially monoenergetic large group of particles will travel a fairly well defined distance through a material before losing their kinetic energy, and hence, stopping. The path length at which half of the particles have been stopped is called the median projected range. Fluctuations in the path length traversed by particles before stopping is known as range straggling.

Since energy loss phenomena of heavy charged particles in matter are influenced by several factors, it becomes convenient to discuss stopping power of a material (defined later) in three different incident particle energy regions.

1. The low energy region, where the energy of the incident particle is less than .5 MeV per nucleon.
2. Intermediate energy region, where the incident particle energy is greater than .5 MeV per nucleon but not extremely relativistic, say less than the particle rest mass energy (Mc^2), as a rather arbitrary

upper bound.

3. High energy region, where particle energies exceed the rest mass energy.

In the low energy region, the incident particle interacts to a great extent with the atoms of the material. Electron capture and loss by positive ions occur and thus the incident particle is fully ionized only part of the time.

In the high energy region, radiative energy loss (bremsstrahlung) will be of importance, as will energy loss due to nuclear reactions. At extremely high energies, much greater than the rest mass energy, the density (or medium polarization) effect becomes important and results in a diminution of the energy loss rate.

In the intermediate energy range, the principal interaction is between the incident particle and the electrons of the constituent atoms comprising the material. This is the region of interest in the present study. Two experiments were performed in this intermediate energy range in which stopping power measurements were made on several materials. Therefore, further discussion will be limited to the case in which the energy of the incident heavy charged particle is within the intermediate energy range.

The stopping power of a material is defined by

$$S = -\frac{1}{\rho}\frac{dE}{dx}$$

where

S = stopping power of the material,

ρ = mass density of the material, and

$\frac{dE}{dx}$ = average rate of energy loss of the charged particle per unit distance traversed through the material.

To explain further, as an energetic heavy charged particle moves through some material, it loses energy in collisions with the electrons of the constituent atoms of the material. This energy serves to excite the atoms to higher energy states or to ionize them. Energy is also lost in nuclear interactions. Although the energy lost per nuclear interaction may be great, these interactions are of such a rare occurrence that the net losses due to nuclear interaction are negligible compared to energy losses incurred in electronic collisions. Stopping power is considered a phenomenon involving directly only the electrons of a material and the incident charged particle. Conservation of momentum and energy permit fractional energy transfers in collisions with electrons of the order of $\frac{m}{M} << 1$, where m is the electronic mass and M is the mass of the incident charged particle. Because the energy lost by the charged particle in a single electronic collision is a small fraction of its total energy, $\frac{dE}{dx}$ can be treated as a continuous function of distance traversed.

Early work on stopping power was initiated by N. Bohr. The currently accepted treatment of stopping power was carried out by H. Bethe and F. Bloch. The account of this work will not be reproduced here. Excellent theoretical discussions of stopping power are given in the works of Fano (1964) and Bichsel (1968). Some aspects of stopping power theory, however, such as approximations and assumptions of limited validity, will be discussed in order to explain more fully the parameters which enter

into the Bethe-Bloch formula for the stopping power of a material, and in order to introduce properly the experimental work which this thesis describes.

The Bethe-Bloch formula for the stopping power of an elemental absorber is (Bichsel, 1968)

$$S = \frac{-1}{\rho}\frac{dE}{dx} = \frac{z^2 Z}{A} K(\beta)\left[f(\beta) - \ln I - \sum_i \frac{C_i}{Z}\right]$$

where

$$K(\beta) = \frac{4\pi e^4 N_o}{mc^2 \beta^2} \qquad f(\beta) = \ln \frac{2mc^2\beta^2}{1-\beta^2} \qquad \beta = v/c$$

and

e = electronic charge

m = electronic rest mass

v = incident particle velocity

c = velocity of light in vacuo

z = atomic number of incident charged particle

Z = atomic number of element

A = atomic mass of element

N_o = Avogadro's number

I = mean excitation energy of element

C_i = shell correction factor for the i^{th} electronic shell of the element (i = K, L, etc.)

The formula, valid in the intermediate energy (or velocity) range, is seen to depend upon several parameters. In any stopping power experiment, all but two of these parameters are generally well known and familiar to physicists. The two exceptions are the mean excitation energy I,

and the shell corrections C_i.

The mean excitation energy I is an important parameter in the stopping power formula. This is a characteristic of the element that the stopping material comprises. It represents a weighted average over the excited energy states of the particular atom, both discrete and continuous. To be exact

$$\ln I = \sum_n f_n \cdot \ln E_n$$

where E_n is the excitation energy of the n^{th} excited state of the atom and f_n is the corresponding oscillator strength for the transition to the n^{th} excited state, including continuum states. The oscillator strength is directly related to the probability of exciting the atom to a particular state.

Very few theoretical I values of elements are known because of lack of knowledge of the oscillator strengths f_n for individual elements. The I values of many elements have been determined experimentally however. The stopping power of an elemental material is generally not very sensitive to small fractional changes in its I value, because of the logarithmic dependence on I. If mean excitation energies are to be derived from measured stopping powers through use of the Bethe-Bloch formula, it is essential to have very accurate stopping power measurements in order to insure that reasonably accurate mean excitation energies are obtained.

In part, the stopping power formula rests on an assumption that the velocity of the incident particle is much greater than that of the atomic electrons in their bound states. This assumption fails at times and leads

to the second parameter mentioned, the shell corrections, C_i. It happens that significant corrections for this approximation are required for the heavier elements at all incident particle energies, and that except for the lightest elements corrections are always required for velocities such that $\beta < 0.4$. For a proton this is an energy of approximately 100 MeV. In most elements, the innermost electrons, i.e., those in the K-, L-, and M-shells of the atom, have sufficient velocities to make the assumption fail. The shell corrections C_i are included in the stopping power formula in order to compensate for this error.

Walske (1952; 1956) has calculated the corrections for the K- and L-shells. These corrections depend upon the velocity of the incident particle and on the stopping element. Corrections for the higher shells have not been calculated, although M-shell electrons are known to contribute significantly to the total correction. At present, mathematical difficulties prohibit calculation of higher shell corrections.

Bichsel (1967), however, has attempted to determine experimentally higher shell corrections, i.e., M- and N-shells, for several elements by assuming that they depend upon the incident particle's velocity in the same way as does the L-shell correction except for some scaling parameters. These scale factors can be determined separately by simultaneous least squares fitting of a large number of experimental stopping power data of various elements to the stopping power formula. Niiler (1969) has since interpolated Bichsel's results to obtain scaling factors for other elements. Bichsel's results appear to be reasonable in that, after fitting, the contribution of each subshell to the total correction is found to depend primarily on the ratio of the particle

velocity to the root mean square velocity of the electrons in the subshell (Fano, 1964; Bichsel, 1968).

Bichsel also developed a Fortran computer program which contains in part a computerized version of Bethe's formula applicable to many different incident particles and for any target material. Bichsel's extension of Walske's L-shell correction to higher shells have been incorporated into this program (Bichsel, 1967).

Another approximation on which the stopping power formula is based is the first Born approximation. This impulse approximation, which leads directly to the projectile z^2 dependence of the stopping power formula, is used to calculate the interaction between the incident particle and the atomic electrons. The second Born approximation leads to an additional term in the formula which is proportional to z^3, the cube of the charge of the incident particle. It is felt that this effect may account for observed differences in stopping powers and ranges of positive and negative particle pairs, such as positive and negative pi mesons. In a very recent paper, this z^3 effect was theoretically accounted for and calculated. The formulation is based on a semi-classical argument considering the interaction of a particle of charge ze at a given impact parameter with an isotropically and harmonically bound electron. Using a perturbation expansion which assumes that electron displacements are small compared to the impact parameter, the total force on the electron can be expressed as the sum of two terms. The first term is exactly that force which leads to the Bethe - Bloch stopping power formula. The other term leads to

a correctional term in the stopping power formula which is proportional to z^3. This term arises in considering distant collisions between the electron and the particle. The z^3 term is evaluated for the Lenz - Jensen statistical model of the atom (Ashley et al., 1972).

The stopping power formula as given applies to any elemental absorbing material. In the case of compounds and other composite materials, the formula is applied assuming the additivity of stopping effects of the constituent elements. The assumption is known as Bragg's rule. The addition is weighted according to the fraction by atom that each constituent element contributes to the whole composite. For a composite then, this rule is expressed by the relations

$$\bar{Z} = \sum_{i=1}^{n} P_i Z_i \qquad \bar{A} = \sum_{i=1}^{n} P_i A_i \qquad \ln I_B = \sum_{i=1}^{n} a_i \ln I_i, \text{ with}$$

P_i = fraction by atom contributed by i^{th} element to the composite,

Z_i = atomic number of i^{th} element, A_i = atomic mass of i^{th} element,

I_i = mean excitation energy of i^{th} element, and

a_i = fraction of total atomic electron population of the composite contributed by the i^{th} element.

The sum extends over the number of different elements in the composite. It should be noted that the average mean excitation energy is a logarithmic average. In the stopping power formula $\bar{Z}$ replaces Z, $\bar{A}$ replaces A, and $\ln I_B$ replaces $\ln I$.

This additivity rule for composites has been shown experimentally to be quite accurate for most composites, even though it neglects the effects of chemical bonds and other aggregation properties associated with composites which modify the stopping power by inducing changes in

the spectra of excited levels of the elements involved. The main reason for its accuracy is that chemical bonds and aggregation properties involve almost exclusively the valence electrons of the elements of the composite, so that only their contribution to the total stopping power is affected. In all but the lightest elements the valence electrons' contribution to the stopping power is but a very small fraction of the total. It has been shown experimentally that the effect of chemical structure on stopping power is of the order of one percent (Fano, 1964). Nevertheless, there are cases of blatant failure of Bragg's rule (Tschalar and Bichsel, 1968; Porter et al., 1970) and in few cases does it obtain exactly. Large discrepancies have thus far not been accounted for.

There is an interesting phenomenon in which the effects of chemical structure on stopping power cannot be claimed to be of the order of one percent. This phenomenon is known as channeling. In certain crystalline materials, such as silicon, energy loss of charged particles in certain directions in the crystal is abnormally low compared to that observed in other directions. These preferred directions are along symmetry planes and axes of the lattice (Erginsoy et al., 1964). The belief is that charged particles incident initially in these preferred directions tend to get "channeled" in these directions by small angle scatterings from the crystal lattice atoms. Electron densities are low along symmetry planes and axes, and hence the particle loses less energy along one of these directions than in a

random direction. Observation of this effect requires careful target preparation and alignment with respect to the incident particle beam. Such steps were not taken in the current experiments, and the shape of the observed spectra accordingly did not indicate that the channeling effect was present.

Stopping power measurements are important for several reasons, three of which are:

1. In nuclear physics experiments, energy losses incurred as particles traverse the experimental apparatus (such as foil windows) must be known accurately in order to obtain meaningful results. In the absence of measured stopping power data, these energy losses must be calculated from Bethe's formula or interpolated from the existing tables of stopping power.
2. The noted failure of Bragg's rule encourages additional stopping power measurements of composite materials in order to investigate more fully this phenomenon.
3. The recent theoretical work on the z^3 effect on stopping power should be experimentally investigated.

The purpose of this study was to provide information on the above three items. Particular attention was given to item number two, pertaining to Bragg's rule.

Two experiments were performed. In the first, deuterons from a vertical Van de Graaff accelerator were used as projectiles. The energy losses of these deuterons as they passed through thin foils made

of Havar, Mu Metal, and Permalloy were measured and used to compute stopping power. All three metals are alloys of well known composition. Havar is widely used as a gas target window, and Mu Metal and Permalloy have possible use as magnetic shielding devices in nuclear physics experiments. Knowledge of energy loss of charged particles in these materials would very likely be of interest in any experimental research utilizing them. In a manner more appropriately described later, a best fit mean excitation energy $\bar{I}$ was ascribed to each alloy through fits of the measured stopping powers with Bichsel's computer code. These $\bar{I}$ values, which are experimentally based, were then compared to those arrived at by applying Bragg's rule. In this way, discrepancies could be attributed to failure of Bragg's rule.

In the second experiment, alpha particles were used as projectiles. These came from a radioactive americium source (^{241}Am). The target foils in this experiment were nickel, aluminum, Mu Metal, Havar, Teflon, and Mylar. The last four materials are composites, the compositions of which are given in Table 8, p. 38 of this thesis. In exactly the same manner as in the deuteron experiment, best fit mean excitation energies were arrived at and compared to the values obtained by application of Bragg's rule. Teflon and Mylar also are employed in nuclear physics experiments. Mylar in particular is used as a window in gas targets and in gas filled counters.

Since the charge of the alpha particle is twice that of the deuteron, the z^3 effect predicts a difference in the deuteron stopping power of Havar and Mu Metal and the alpha particle stopping power of Havar and Mu Metal

which is not attributable to the Bethe-Bloch stopping power formula. The comparison was made, but no conclusions were drawn from it because of imprecision of experimental data, as will also be explained below.

CHAPTER II

THE DEUTERON EXPERIMENT

The experimental arrangement is diagrammed in Figure 1. A monoenergetic beam of deuterons from the Los Alamos Scientific Laboratory Vertical Van de Graaff Accelerator entered the circular chamber and impinged normally upon a gold foil of areal density $200 \mu \frac{gm}{cm^2}$ located at the center of the chamber. Deuterons scattered forward and upward at an angle of 39° with respect to the line formed by the incident beam passed through various target foils and into a detector after traversing a collimator system.

The upper half of the circular chamber rotated atop the lower half. This upper half of the chamber was outfitted with a target foil holding device, a collimating tube, an adjustable slit, and an Ortec E-015-100-100 Detector with housing. The collimator was about 10 cm long and protruded through the cylindrical wall of the chamber with its long axis at an angle of 39° above the horizontal. The collimator was situated partially inside and partially outside the chamber. The slit and the detector were attached to the outside end of the collimator. A brass frame about 5 cm in length was fabricated for this experiment to hold the target foils. The frame, attached to the inside end of the collimator, extended to within 5 cm of the gold foil. The entire assembly was rotated so that its long axis lay in the same vertical plane which contained the deuteron beam, and was elevated 39° above

FIGURE 1

DEUTERON EXPERIMENTAL ARRANGEMENT

Top View

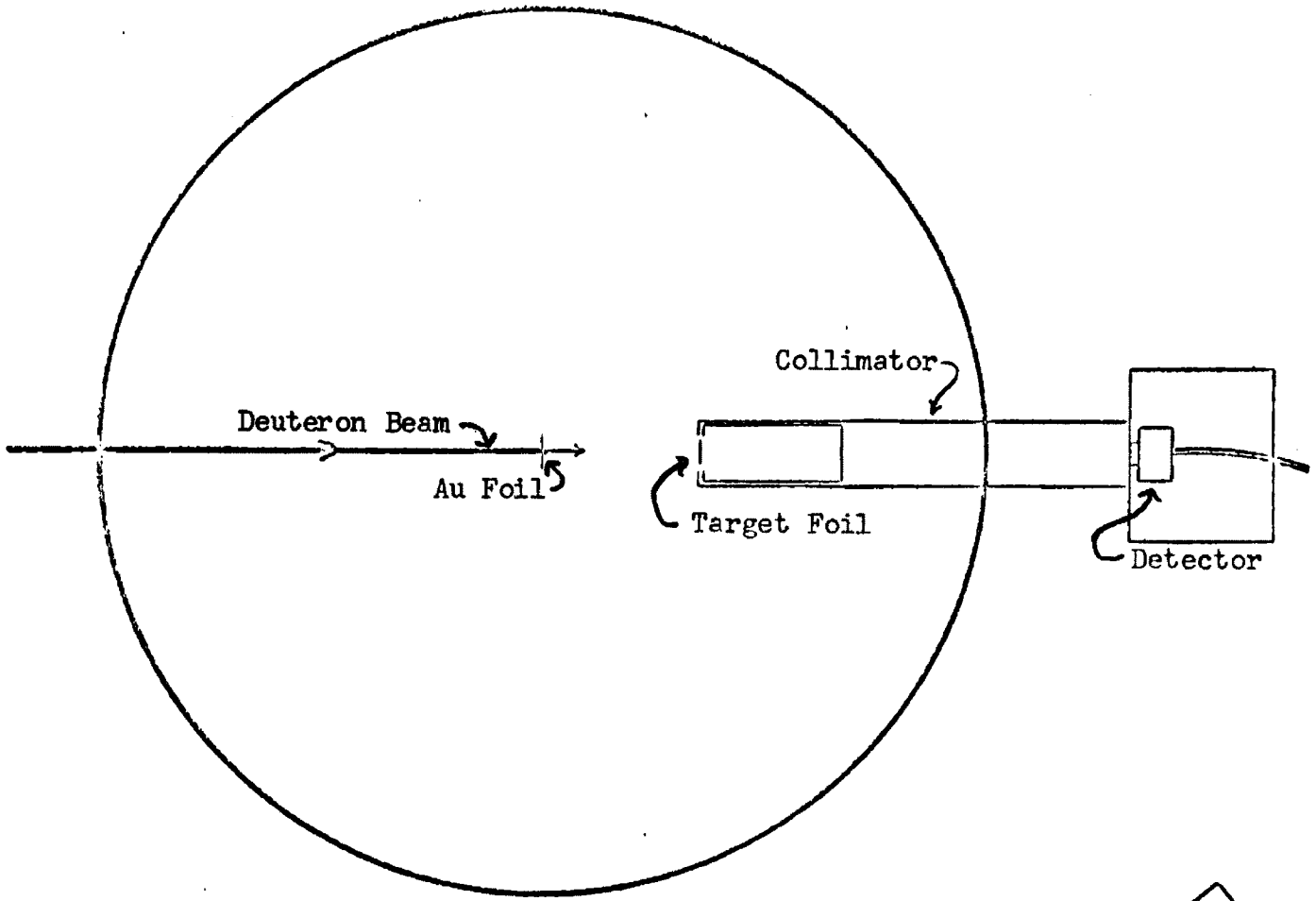

Side View

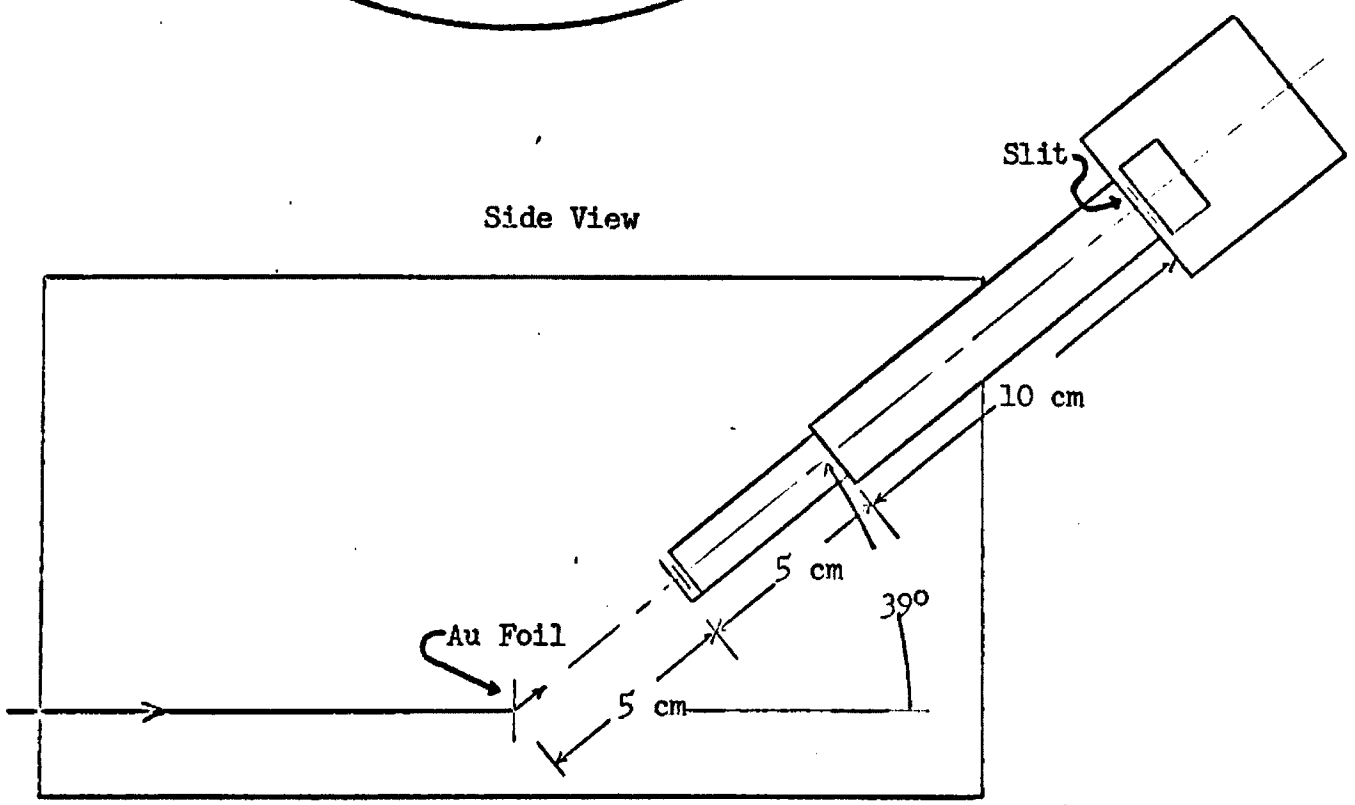

the horizontal with the vertex of the angle at the center of the gold foil. Therefore, deuterons scattered forward and 39° upward from the gold foil impinged normally on the particular target foil in the foil holding device, passed through this foil and through the collimator system and penetrated into the detector, where they were stopped. The signals thus generated in the detector were fed through a preamplifier, a linear amplifier, and finally into a 400 channel pulse height analyzer.

The experiment was conducted in the following manner: First the linear amplifier gain was adjusted so that 5.48 MeV alpha particles caused pulses near channel 350 of the analyzer. The accelerator was tuned so as to deliver 2.42 MeV deuterons at the chamber entrance. The chamber, including the collimator and detector assembly, was evacuated to a very low pressure comparable to the pressure of the deuteron beam tube (about 5×10^{-6} mm Hg.). The first run was made with no foil in place.

Data were allowed to accumulate for about ten minutes and a paper tape readout from the analyzer showing the number of counts in each of the 400 channels was taken. The deuteron beam was then diverted and the beam tube was sealed by means of a valve. Air was let back into the scattering chamber. A .004 millimeter thickness Havar foil was inserted into the foil holder and the chamber was again evacuated. The next run was made with this foil as the target. The above procedure was repeated for target foils of .006 mm thickness Mu Metal, .006 mm thickness Permalloy and .008 mm thickness Havar in that order, and at the same beam energy of 2.42 MeV. The beam energy was increased to 3.50 MeV and runs were repeated with the same four foils as targets. A final run at

3.50 MeV deuteron energy was made with no foil in place.

The channel pulse heights on the paper tape readouts were plotted on graph paper and first moment calculations were performed in order to determine the peak locations of the spectra to the nearest tenth of a channel.

$$\text{Peak location} = \sum_{i=m}^{n} N_i \cdot i \Big/ \sum_{i=m}^{n} N_i$$

where N_i is the number of counts in channel number i and the sum extends over the particular spectrum. Table 1 lists the beam energy, the target foils, and the corresponding peak locations. An uncertainty of $\pm \frac{1}{2}$ channel was assigned to the peak locations of the spectra.

The two runs made with no foil in place were used to establish the detector system calibration curve. This curve is plotted in Figure 2. With this curve, the energy losses incurred by the deuterons in traversing the various foils could be determined by knowing the peak locations of each of the spectra.

In plotting the calibration curve and determining the energy losses of deuterons traversing the target foils, the energy lost by the deuterons during transmission through the gold foil was taken into account. These losses, due to the stopping power of the gold foil and Rutherford nuclear scattering at 39°, were 25 keV and 27 keV for the beam energies 2.42 MeV and 3.50 MeV, respectively. Table 2 displays the foils, and energy losses of deuterons in them along with the experimental uncertainties, discussed in a later section.

Knowledge of the areal densities of the target foils (M/A) and

the energy losses of the deuterons in each of the target foils (ΔE) allowed determination of the stopping power for each target foil from the equation

$$S(E) = \frac{\Delta E}{(M/A)}$$

In each individual foil the energy at which the stopping power is thus experimentally determined was taken to be very nearly the energy equal to the incident deuteron energy minus one-half the total energy loss in the foil. Assuming linearity of the stopping power curve as a function of energy for these total energy loss intervals, these central energies would be those that the deuterons would possess halfway through each of the foils. For larger energy losses, say greater than twenty percent of the initial deuteron energy, this approximation is not sufficiently precise and a slight correction must be made. This correction is discussed in a later chapter of this thesis. Table 3 gives the stopping powers of all foils and the energies at which determined, with the experimental uncertainties.

FIGURE 2

ENERGY CALIBRATION - DEUTERON EXPERIMENT

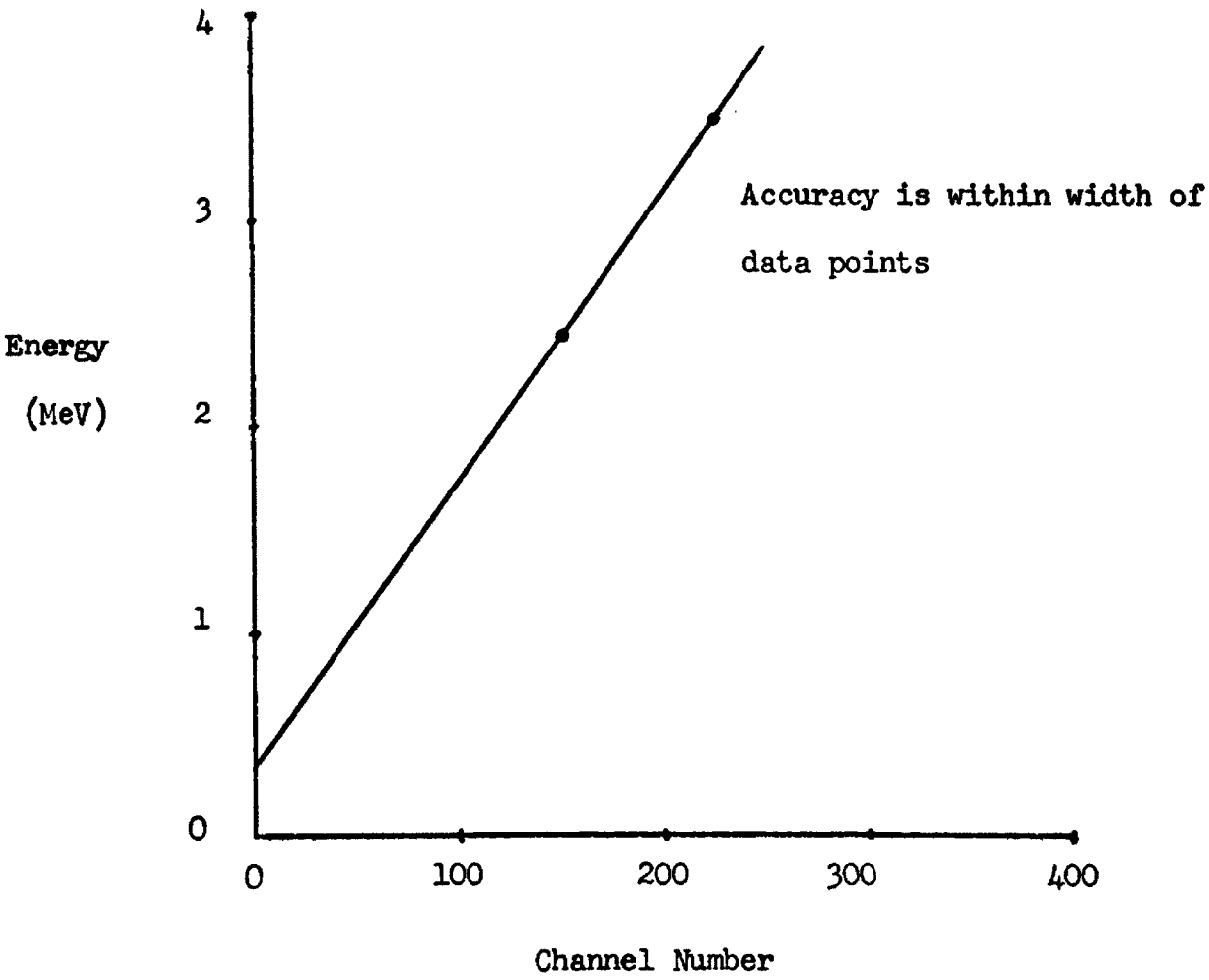

TABLE 1

DEUTERON PULSE HEIGHT SPECTRA PEAK LOCATIONS

Target Foil	Nominal Thickness (10^{-4}cm)	Machine Energy (MeV)	Channel	Uncertainty (keV)
Havar	8.4	2.42	93.7	7.5
Havar	3.8	2.42	123.3	7.5
Mu Metal	6.4	2.42	99.7	7.5
Permalloy	6.4	2.42	102.7	7.5
No Foil		2.42	148.7	7.5
Havar	8.4	3.50	178.7	7.5
Havar	3.8	3.50	200.3	7.5
Mu Metal	6.4	3.50	182.6	7.5
Permalloy	6.4	3.50	184.6	7.5
No Foil		3.50	220.1	7.5

TABLE 2

ENERGY LOSSES

Target Foil	Nominal Thickness (10^{-4}cm)	Machine Energy (MeV)	Energy Loss (MeV)	Uncertainty (keV)
Havar	8.4	2.42	.831	10.6
Havar	3.8	2.42	.384	10.6
Mu Metal	6.4	2.42	.742	10.6
Permalloy	6.4	2.42	.695	10.6
Havar	8.4	3.50	.626	10.6
Havar	3.8	3.50	.296	10.6
Mu Metal	6.4	3.50	.568	10.6
Permalloy	6.4	3.50	.537	10.6

TABLE 3

DEUTERON STOPPING POWERS

Target Material	$E_1 \simeq E_o - \frac{\Delta E}{2}$ (MeV)	Stopping Power $S(E_1)\left(\frac{\text{MeV} \cdot \text{cm}^2}{\text{gram}}\right)$	Uncertainty (Δ S) $\left(\frac{\text{MeV} \cdot \text{cm}^2}{\text{gram}}\right)$
Havar	1.936 ± .017	127	2.2
Havar	2.165 ± .016	119	3.8
Havar	3.136 ± .017	95.6	1.9
Havar	3.325 ± .017	91.5	3.3
Mu Metal	1.964 ± .017	130	2.6
Mu Metal	3.180 ± .017	99.3	2.3
Permalloy	1.998 ± .017	135	2.7
Permalloy	3.192 ± .017	105	2.6

CHAPTER III

ALPHA PARTICLE EXPERIMENT

This experiment used alpha particles as projectiles. These alpha particles came from a radioactive americium source (^{241}Am) which was plated onto a tantalum backing in a dioxide compound (AmO_2). The source had a thin line geometry, approximately .46 cm long, .0025 cm wide, and .0032 cm in depth. The source mass was 0.53 micrograms.

^{241}Am decays only by alpha particle emission. The two principal decay modes yield alpha particles of energies 5.486 MeV and 5.443 MeV. 86% of all alpha particles are emitted with the former energy and 12.7% are emitted with the latter energy. A multitude of lower energy decay modes account for the remainder of the alpha particles, about 1.3%. The half life of ^{241}Am is 458 years. The daughter product formed from ^{241}Am after emission of an alpha particle is ^{237}Np. This isotope also decays only by alpha emission with a half life of 2.16×10^6 years. Hence this daughter element contributes an entirely negligible amount to the total alpha particle count. That is, the ^{241}Am alpha particle energy spectrum is not affected by the presence of this daughter element.

The experimental arrangement and equipment are diagrammed in Figure 3. The ^{241}Am source was mounted on the vertical portion of an L-shaped assembly by means of an open plate which left the line source

FIGURE 3

ALPHA PARTICLE EXPERIMENTAL ARRANGEMENT

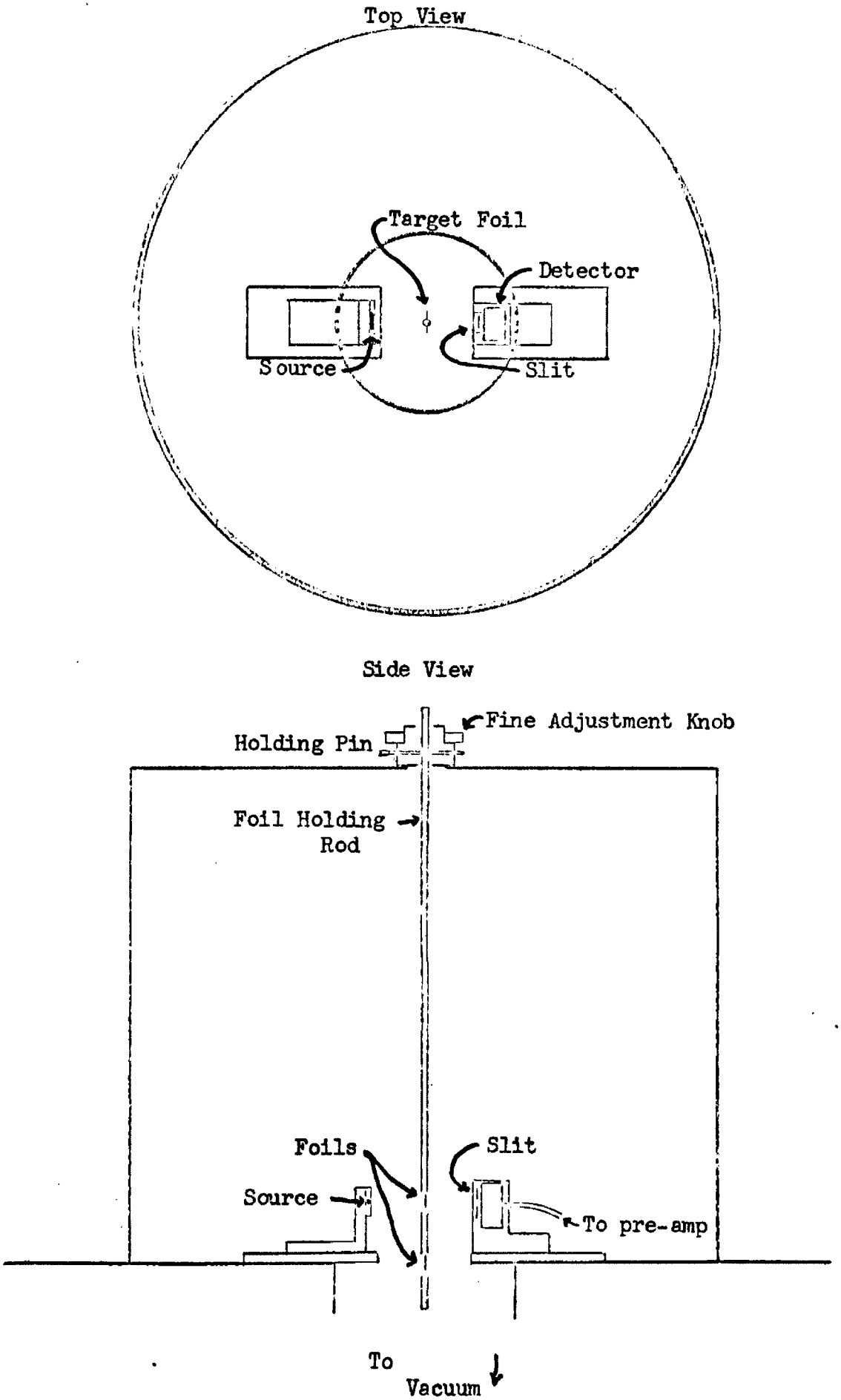

exposed. A slit and detector assembly was positioned directly opposite the source and aligned so that the line source was centered on the slit. The line source was adjusted so that it was horizontal. The detector slit separation in the vertical direction was set at .64 cm. The horizontal width of the slit was .51 cm. The distance between source and slit was set at 3.8 cm. Directly behind the slit was an Ortec E-015-100-100 Detector.

A large brass cylinder, open on one end, was placed over the above equipment and onto the circular plate upon which this equipment was centered. This assembly formed the vacuum chamber for the experiment. On top of the cylinder and at the center was a circular opening into which fit the target foil holding assembly. With this assembly, the target foils, attached along the length of a straight rod, were lowered into the chamber between the source and slit. The construction of the foil-holder device permitted adjustments to be made throughout the experiment so that the foil plane was always parallel to the line source and slit-plane, and centered on the line from source center to slit center. A vacuum pump evacuated the chamber through a hole in the center of the bottom circular plate. Pressures of about 7 microns of mercury were maintained throughout the experiment.

In operation, alpha particles from the ^{241}Am source passed through the target foils and through the .64 cm x .51 cm rectangular slit opening and then penetrated the detector, where they were stopped. Signals thus generated within the detector were fed into a preamplifier, a linear amplifier, and finally a Nuclear Data 1024 channel analyzer.

An oscilloscope was used to observe the amplified signals. Data readout from the analyzer was in the form of Polaroid photographs depicting the number of counts in each of the 1024 channels.

Prior to data gathering the linear amplifier gain was set so that 5.5 MeV alpha particles caused pulses near channel 1000. Measurements of energy loss were made on the following target foils:

.0006 mm, .001 mm, .002 mm, .004 mm nickel

,003 mm Mu Metal

.005 mm aluminum

.002 mm .004 mm. Havar

.006 mm Mylar

.006 mm Teflon

The procedure in collecting data was first to load the foils into the foil-holding rod, then to lower this assembly into the chamber, and to align it. The chamber was then evacuated. A 60 volt bias was placed across the detector and data were allowed to accumulate for about one and one-half hours. After this time a readout of the data was taken and another foil was lowered into position and the procedure was repeated. The foil-holding device held no more than three foils. After measurements were taken on all the foils in the holder, air was let back into the chamber, another set of foils was loaded into the foil-holder and the procedure was repeated. One measurement was taken with no foil between the source and detector. Two measurements were made on each of the foils of composite materials. Single measurements were made on the elemental foils.

The spectrum for each run was plotted on graph paper from the numbers indicated on the photographs. The aforementioned 12.7% low energy alpha particle spectrum due to the ^{241}Am decay mode at 5.443 MeV was subtracted out of each spectrum. Using the resulting graphs, the peak locations for the higher energy alpha particle spectra were determined for each data run to the nearest tenth of a channel by performing first moment calculations. In each individual case,

$$\text{Peak location} = \sum_{i=m}^{n} N_i \cdot i \Big/ \sum_{i=m}^{n} N_i$$

where N_i is the number of counts in channel number i and the sum extends over the spectrum. An uncertainty of $\pm$ 1.5 channels was assigned to the peak locations. Table 4 lists the foils and channel peak locations along with the uncertainties.

The measurement with no target foil in place, along with the measurements on the nickel foils and the aluminum foil, provided the energy calibration curve for the analyzer. This calibration was done in the following manner:

1. The run with no foil in place established the uppermost point of the calibration curve, which was assumed linear. In this case channel 1009.5 corresponded to an energy of 5.427 MeV.
2. Assuming a slope value of approximately 5.4 keV/channel, which corresponds to channel number zero having zero energy, the energy loss in each of the nickel foils and in the aluminum foil was calculated from knowledge of the channel in which the peak

of the spectrum of each foil was located, and the energy of channel 1009.5.

3. These energy losses were divided in half and subtracted from the incident alpha particle energy, 5.427 MeV, to obtain the energies of the alpha particles halfway through the nickel foils or the aluminum foil. Values of stopping power with alpha particles as projectiles at these energies were then interpolated from stopping power curves generated by Bichsel's computer code. The curves for nickel and aluminum should be highly reliable since the input parameter values are based on many measurements of stopping power of nickel and aluminum.

4. With these stopping powers, the energy losses that should have occurred for these nickel and aluminum foils were calculated from

$$\Delta E = S \cdot M/A$$

and compared to the previously mentioned values obtained by assuming approximately 5.4 keV/channel. Some discrepancy is expected due to experimental errors in determining peak locations and in measuring the areal densities of the foils (M/A). A best fit energy per channel was then determined by varying the energy per channel until the differences between observed and calculated energy losses were reduced to a minimum in a least squares sense. That is, a single parameter linear regression was performed on these data points. The standard error for the energy per channel arrived at (5.475 keV/channel) was calculated to be 1.2 per cent.

TABLE 4

ALPHA PARTICLE PULSE HEIGHT SPECTRA PEAK LOCATIONS

Target Foil	Nominal Thickness (10^{-4}cm)	Channel	Uncertainty (keV)
Aluminum	5.1	856.3	8.1
Havar	2.3	851.4	8.1
Havar	3.8	740.4	8.1
Mu Metal	3.2	779.2	8.1
Mylar	6.4	877.5	8.1
Nickel	.64	956.9	8.1
Nickel	1.3	917.4	8.1
Nickel	2.6	820.9	8.1
Nickel	2.6	803.5	8.1
Nickel	3.8	737.5	8.1
Teflon	6.4	835.8	8.1
No Target		1009.5	7.5

A graph of the best fit calibration line is included in Figure 4. Having established this line, the energy losses incurred by alpha particles in traversing the other foils could then be determined. Table 5 lists the foils, the energy losses, and the experimental uncertainties of the energy losses.

In the same manner as described in the deuteron experiment, these energy losses yield immediately the experimental stopping power for each foil. Table 6 shows the stopping powers of all materials at the specified energies and also lists the experimental uncertainties. Typical deuteron and alpha particle pulse height spectra are shown in Figures 5 and 6, respectively.

FIGURE 4

ENERGY CALIBRATION - ALPHA PARTICLE EXPERIMENT

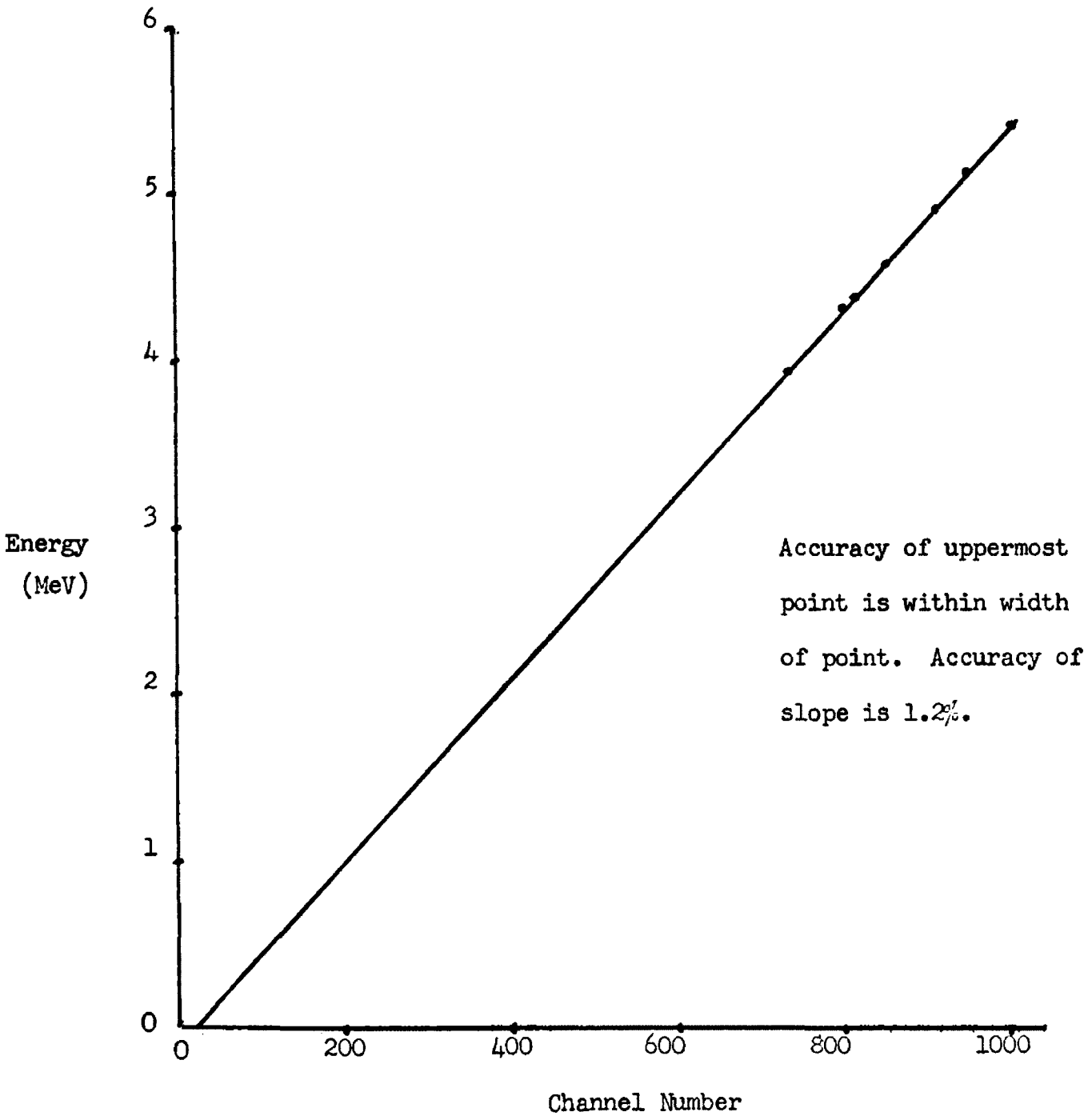

TABLE 5

ENERGY LOSSES

Foil	Nominal Thickness (10^{-4}cm)	Energy Loss (MeV)	Uncertainty (MeV)
Havar	2.3	.866	.014
Havar	3.8	1.473	.020
Mu Metal	3.2	1.261	.018
Mylar	6.4	.723	.013
Teflon	6.4	.951	.015

TABLE 6

ALPHA PARTICLE STOPPING POWER

Target Material	$E_1 \cong E_o - \frac{\Delta E}{2}$ (MeV)	Stopping Power $S(E_1)$ $\left(\text{MeV} \cdot \frac{\text{cm}^2}{\text{gram}}\right)$	Uncertainty $\left(\text{MeV} \cdot \frac{\text{cm}^2}{\text{gram}}\right)$
Havar	4.542 ± .016	456	7.92
Havar	4.970 ± ..010	438	8.51
Mu Metal	4.724 ± .012	468	9.29
Mylar	5.059 ± .009	807	16.6
Teflon	4.930 ± .010	665	12.5

FIGURE 5

TYPICAL DEUTERON SPECTRUM

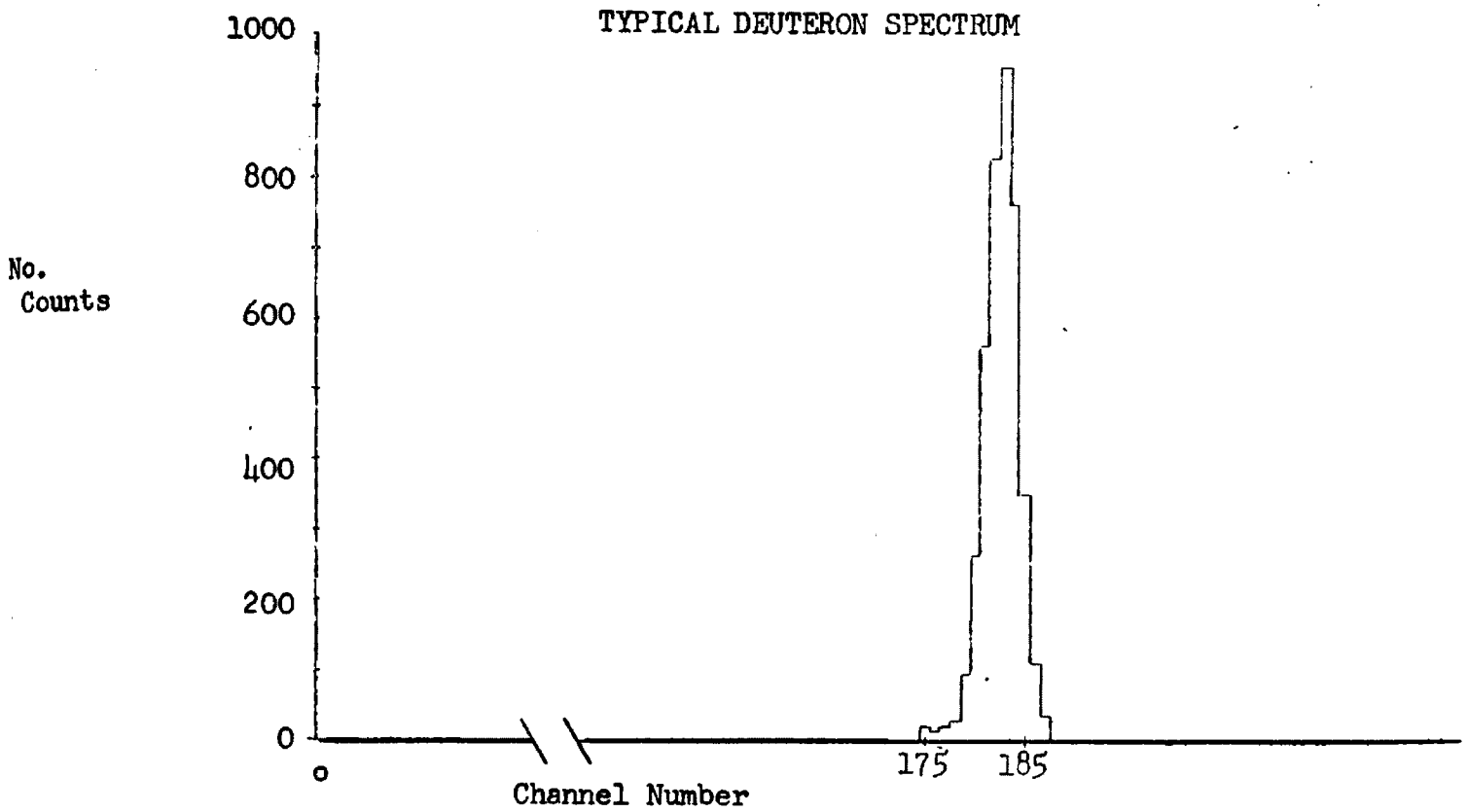

FIGURE 6

TYPICAL ALPHA PARTICLE SPECTRUM

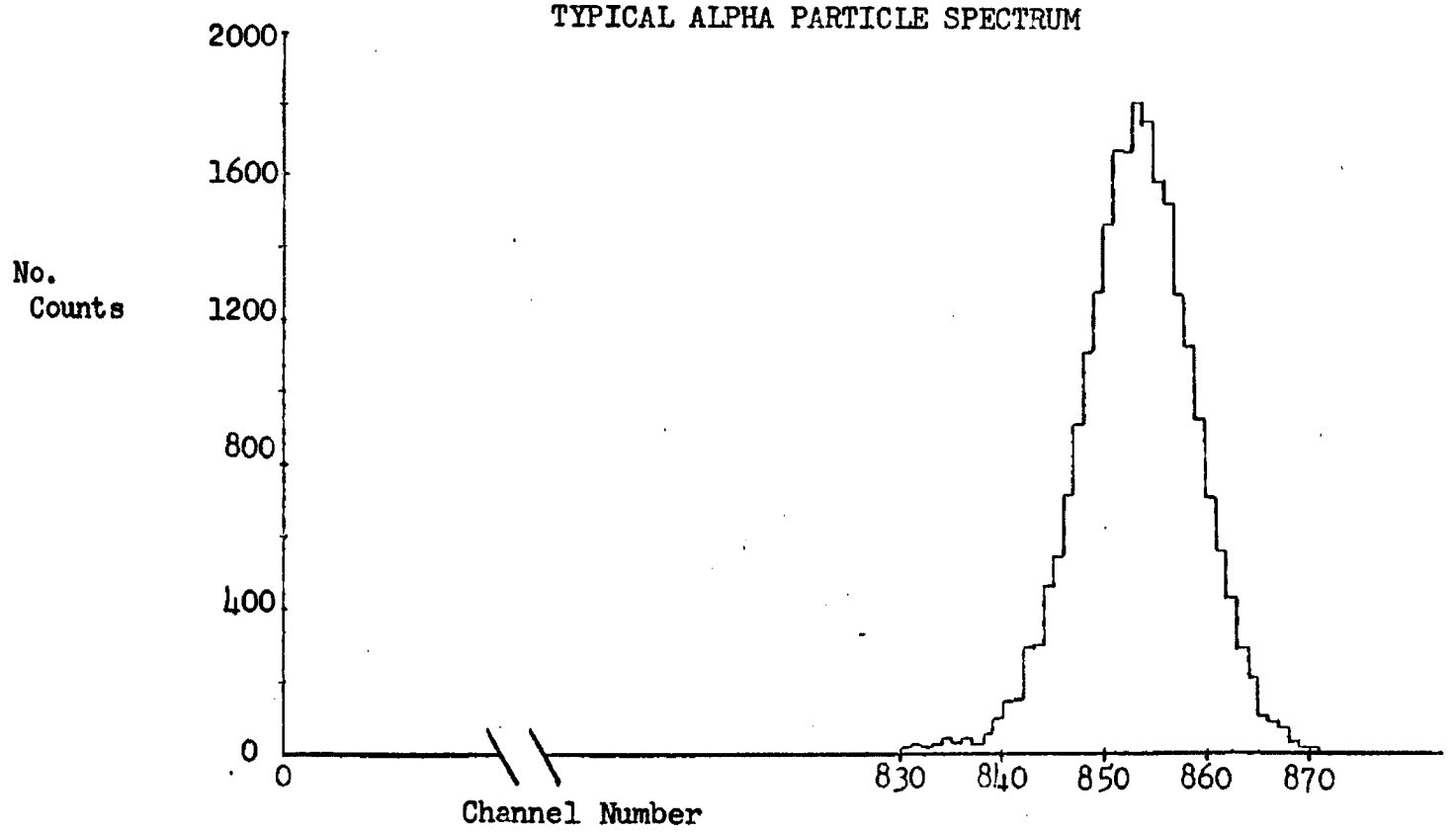

CHAPTER IV

FOIL PREPARATION

The target foils for these experiments were prepared in the following manner. Very nearly rectangular foils were cut from existing larger foil sections using a razor blade. After mass and area measurements were made on the foils, they were mounted in standard foil holders for experimental use.

The area of the foil was measured in each case by placing the foil on a glass plate and overlaying the foil with semi-transparent fine grid (400 squares per square inch) linear graph paper. The area was then determined from the area of the graph paper under which lay the foil. Because the foils were very nearly rectangular and the grid of the graph paper was small, areas were estimated to be accurate to within one per cent.

The masses of the foils were measured using a Cahn electrobalance, which permits accuracies to within one half per cent.

The area A and mass M and M/A for each of the foils are listed in Table 7. The compositions of the foils are given in Table 8.

The degree of the uniformity of the foils used is not known. In both experiments relatively large areas of the target foils were exposed to the incident particles, tending to average out any non-uniformity in the thickness of the foils. This is particularly true in the

alpha particle experiment and consequently foil thickness non-uniformity is not believed to be a problem in this experiment. Internal consistency of the data in the deuteron experiment along with consistency with the results of the alpha particle experiment indicate that the Havar and Mu Metal foils used in the deuteron experiment were very uniform. No such check is possible with the Permalloy foil, since only one foil was used in the deuteron experiment and no measurements were made on Permalloy with alpha particles as projectiles. Therefore foil thickness non-uniformity cannot be conclusively discounted as a possible influence in the results obtained for Permalloy.

TABLE 7

FOIL THICKNESS DATA

Foil	Nominal Thickness (10^{-4}cm)	Area, A (cm^2)	Mass, M (10^{-3} gm)	M/A ($10^{-3}\frac{gram}{cm^2}$)
Aluminum	5.1	5.56	7.84	1.41
Havar	2.3	3.56	7.05	1.98
Havar	3.8	3.60	11.6	3.23
Havar	8.4	3.58	23.4	6.55
Mu Metal	3.2	3.21	8.64	2.69
Mu Metal	6.4	3.58	20.5	5.72
Mylar	6.4	3.58	3.22	.899
Nickel	.64	3.00	1.96	.655
Nickel	1.3	3.60	4.18	1.16
Nickel	2.6	3.61	8.36	2.31
Nickel	2.6	4.13	10.1	2.44
Nickel	3.8	5.26	16.9	3.21
Permalloy	6.4	3.56	18.6	5.28
Teflon	6.4	5.15	7.41	1.44

Uncertainty in M/A for all foils except Mu Metal and Permalloy is 1.1 per cent. For Mu Metal and Permalloy, the uncertainty in M/A is 1.4 per cent.

TABLE 8

FOIL COMPOSITION

Material	Elements of Material and Percent Composition by Weight
Havar	Beryllium(0.04), Carbon (0.20), Chromium (20.0), Manganese (1.60), Iron (17.5), Cobalt (42.5), Nickel (13.0), Molybdenum (2.40), Tungsten (2.80).
Mu Metal	Chromium (2.0), Copper (5.0), Iron (18.0), Nickel (75.0).
Permalloy 4750	Iron (52.7-49.7), Nickel (47-50), Manganese (0.03)

Mylar is a compound, the formula of which is $C_{10}H_8O_4$.

Teflon is a compound, the formula of which is $(C_2F_4)_n$.

CHAPTER V

ERROR ANALYSIS

Deuteron Experiment

For a deuteron beam of energy E_o incident upon a target foil of mass M and area A, and transmitted with an energy loss ΔE, the measured stopping power at an energy very nearly $E_1 \cong E_o - \frac{\Delta E}{2}$ is given by $S(E_1) = \frac{\Delta E}{M/A}$

Here A, M, and ΔE are measured quantities. If errors in measuring these quantities are uncorrelated and random, as will be assumed hereafter, the fractional uncertainty $\frac{\Delta S}{S}$ in the stopping power is given by

$$\frac{\Delta S}{S} = \sqrt{\left(\frac{\Delta A}{A}\right)^2 + \left(\frac{\Delta M}{M}\right)^2 + \left(\frac{\Delta(\Delta E)}{\Delta E}\right)^2}$$

In all cases, the area measurements are believed to be accurate to within 1%. This belief is justified by the method used to prepare foils and measure foil areas as previously described. Operationally, area measurements taken on three different occasions by the same person substantiate this estimate of accuracy.

The masses of the foils were measured with a Cahn electrobalance which, when calibrated and properly used, measures masses to .1%. Tests of the electrobalance with standard weights certified as highly accurate (Class M) by the National Bureau of Standards showed the

electrobalance to be accurate to within .5%.

The foil masses, which were measured on two different occasions, showed a high degree of reproducibility. All indications are that the masses are accurate to within .5% in all cases except for the Mu Metal and Permalloy foils. In these cases, larger dispersions in multiple measurements imply that 1.0% is a more reasonable assigned uncertainty.

The uncertainty in determining the energy losses ΔE is dependent almost entirely on the channel width for the 400 channel pulse height analyzer, which was 15.1 keV per channel. Peak locations were determined to the nearest tenth of a channel, and an uncertainty of $\pm \frac{1}{2}$ channel (i.e., $\pm$ 7.5 keV) was assigned to this peak location to reflect the pulse height resolution of the analyzer. The uncertainty in any energy loss measurement $\Delta(\Delta E)$ is then due to uncertainties in the peak locations of the unretarded and retarded beams.

$$\Delta(\Delta E) = \sqrt{(7.5 \text{ keV})^2 + (7.5 \text{ keV})^2} = \sqrt{2} \cdot 7.5 \text{ keV} = 10.6 \text{ keV}$$

and, hence,

$$\frac{\Delta S}{S} = \sqrt{(.01)^2 + (.01)^2 + \left(\frac{10.6 \text{ keV}}{\Delta E \text{ (keV)}}\right)^2} \quad \text{for Mu Metal and Permalloy}$$

$$\frac{\Delta S}{S} = \sqrt{(.01)^2 + (.005)^2 + \left(\frac{10.6 \text{ keV}}{\Delta E \text{ (keV)}}\right)^2} \quad \text{for Havar}$$

Uncertainties arise in determining the energies at which the stopping powers of this experiment are measured. An uncertainty of ±15 keV was assigned to the analyzed beam energy of the accelerator used in this experiment (Henkel, 1973). Accuracy of the central energy rests on the most recent calibration, which occurred about two years

prior to this experiment.

The calculated energy loss incurred by the deuteron beams in transmission through and scattering within the gold foil is assumed accurate within ±3 keV. For a total calculated energy loss for these effects of 27 keV, this is a liberal uncertainty of 11 per cent. This uncertainty results mostly from lack of precise knowledge of areal density of the gold foil, which was given to be 200 $\frac{\mu gm}{cm^2}$ (Gursky, 1973). Let ΔE_B be the uncertainty in beam energy, ΔE_G be the uncertainty in the energy loss due to traversing the gold foil, and, as before, $\Delta(\Delta E)$ be the uncertainty in the energy loss due to traversing the target foil. The uncertainty in determining the energy at which a stopping power measurement is made is given by

$$\Delta E_1 = \sqrt{(\Delta E_B)^2 + (\Delta E_G)^2 + \left[\frac{\Delta(\Delta E)}{2}\right]^2}$$

$$\Delta E_1 = \sqrt{(15\ \text{keV})^2 + (3\ \text{KeV})^2 + (5.3\ \text{keV})^2} = 16.2\ \text{keV}$$

The stopping formula

$$S(E_1) = \frac{A}{M} \cdot \Delta E \qquad \text{where } E_1 \cong E_o - \frac{\Delta E}{2}$$

assumes that the stopping power curve as a function of energy is linear throughout the energy interval ΔE. For large energy losses, say 20 per cent or more of the incident energy, this approximation is not sufficiently precise, and the assumed linear stopping power curve lies above the true stopping power curve as the diagram immediately below illustrates.

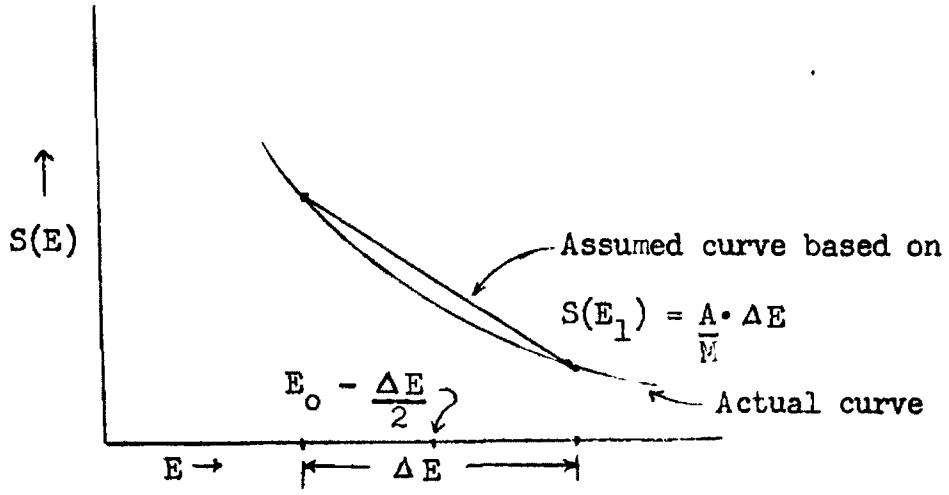

The diagram shows that the assumed stopping power at $E_o - \frac{\Delta E}{2}$ is higher than the true stopping power. However, it is the correct stopping power at an energy slightly less than $E_o - \frac{\Delta E}{2}$, about 1% of ΔE. The desired procedure is then to shift the energy from $E_o - \frac{\Delta E}{2}$ to the correct value. The energy correction to be made can be estimated very closely by observing from the stopping power graph of an element very close (in stopping power) to the target in question the necessary correction to be made if a deuteron beam had suffered an identical energy loss with an identical incident energy in that element.

In the case of Havar, Mu Metal, and Permalloy, a stopping power curve for nickel was used to obtain the correction. Errors made in utilizing this method are within 10% of the correction factor. This error is due almost entirely to errors in drawing the nickel graph and in measuring the energy shift from the graph. The uncertainties in E_1 shown in Tables 3 and 6 have this uncertainty taken into account. For deuterons, the uncertainty in E_1 becomes

$$\Delta E_1 = \sqrt{(16.2 \text{ keV})^2 + (0.1 \times \text{correction factor})^2}$$

Alpha Particle Experiment

The fractional uncertainty in the stopping power is, as in the deuteron experiment, given by

$$\frac{\Delta S}{S} = \sqrt{\left(\frac{\Delta A}{A}\right)^2 + \left(\frac{\Delta M}{M}\right)^2 + \left(\frac{\Delta(\Delta E)}{\Delta E}\right)^2}$$

The area and mass measurements of the target foils are of the same precision as in the deuteron experiment.

The uncertainty in the energy losses ΔE is complicated by several factors. As mentioned in the introduction of this paper, the energy calibration curve for the 1024 channel pulse height analyzer (Figure 3) was arrived at by least squares fitting of five nickel data points and the aluminum data point. This linear regression showed that the channel width (i.e., energy per channel) of the analyzer was 5.475 $\pm$ .070 keV/channel. This result implies that the energy difference between any channel and channel 1009.5, the channel in which the peak of the unretarded alpha particles lay, is uncertain by 1.2% due to the regression line uncertainty above.

There exists an uncertainty in assigning peak locations to the data spectra. These peak positions were calculated to the nearest tenth of a channel. The resolution of the detector was found to be 7.5 keV (half-width at half-maximum for the unretarded spectrum), which corresponds to approximately 1½ channels. The basic uncertainty in all peak locations is then taken to be 1½ channels, or 7.5 keV, in accordance with this resolution.

In all of the retarded alpha particle spectra, the 5.443 MeV ^{241}Am

alpha particle activity, which constitutes about 13% of the total activity, had to be subtracted out of the total spectra before it was possible to determine peak locations for the higher activity, which is the only one of interest. As these two activities became unresolvable when the alpha particles passed through any foil, the following method was used to subtract the background activity in each case.

1. The location of the principal activity peak was guessed at from the shape of the spectrum. All of the spectra had well resolved peaks so that this guess was certainly accurate to within 2 channels.
2. From this guessed principal activity peak, the position of the lower activity peak was determined to be at the position which was 8 channels lower in energy. This step follows because the energy difference between the two activities is only 43 keV, approximately 8 channels, and so alpha particles from both activities would lose virtually the same amount of energy upon passage through any foil. Hence, their energy difference would still be 43 keV after passage through the foils.
3. The height of the lower peak is about 15% of the height of the principal peak, from the ratio of their activities $\left(\frac{.13}{.87} \simeq .15\right)$. Since the height of the principal peak is observable, the height of the lower peak is deduced. The full-width at half-maximum for both activities is the same and, in general, the widths of both activities are the same at any fraction of the total height. The half width at half maximum for the principal peak is observable

and can be accurately estimated to within a channel. This gives the half width at half maximum for the lower peak. Approximate symmetry of the spectrum gives the full width at half maximum.

4. From these deduced three points of the spectrum of the lower activity (the peak position and the two points at half-maximum), the shape of the lower activity spectrum is fairly well determined and can be drawn on the graph of the total spectrum. It becomes an elementary matter to subtract it out.

The above subtraction procedure is subject to error because of the estimates that have to be made. To test for the magnitude of this error, the lower activity spectrum for a nickel plot was subtracted in two different ways. In the first, the peak position of the lower activity was moved to about $5\frac{1}{2}$ channels from the apparent higher activity peak. Visual inspection showed that the resulting lower activity spectrum could not possibly be displaced farther in this direction. In the second plot, the lower activity peak location was moved to about $10\frac{1}{2}$ channels away from the apparent higher activity peak. Visual inspection of this spectrum showed that it could not be displaced farther in this direction. The difference in the peak locations of the principal activity after subtracting first one extreme and then the other was nearly one channel. The uncertainty in the principal peak locations for all foils after subtraction of a best guess lower activity, more reasonable than the extremes mentioned above, was taken to be $\pm \frac{1}{2}$ channel, or 3.0 keV. (Figure 7 is a visual aid to the above discussion.)

FIGURE 7

BACKGROUND SUBTRACTION

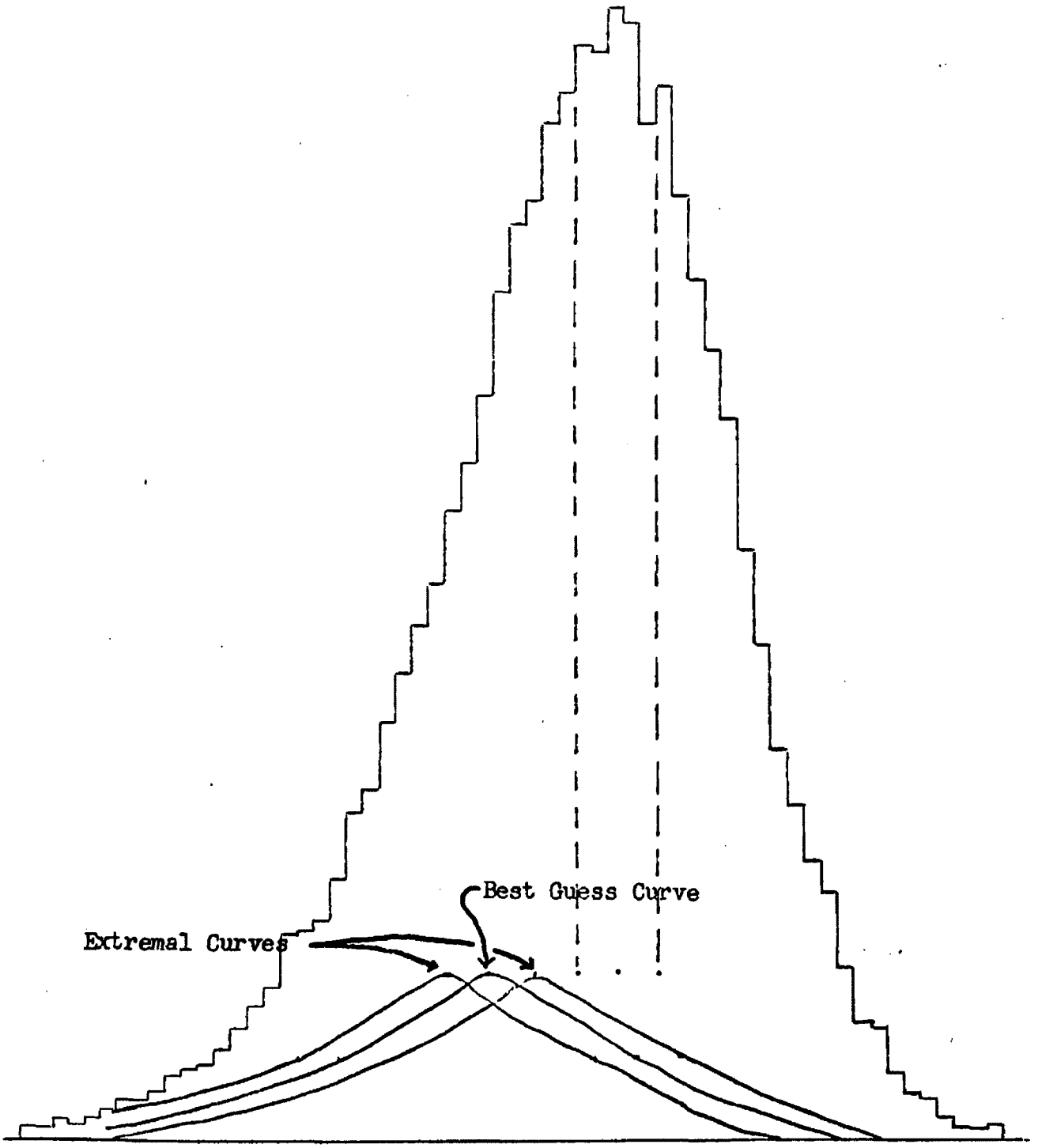

The various contributions to the overall uncertainty in energy loss in view of the preceding discussions are:

1. Basic uncertainty in peak locations of the unretarded peaks and retarded peaks, $\pm$ 7.5 keV in both cases.
2. Uncertainty, due to channel width uncertainty, in the energy assigned to the retarded peak locations, $\pm$ (0.012) (Δ E).
3. Uncertainty in background subtraction, $\pm$ 3.0 keV.

Then, $\Delta(\Delta E) = \sqrt{(7.5 \text{ keV})^2 + (7.5 \text{ keV})^2 + (3.0 \text{ keV})^2 + (.012\Delta E)^2}$

Two spectra were taken for each of the foils, and the average of these was taken to be the energy loss. By having two spectra for all targets, the uncertainty in the peak locations of the retarded spectra is reduced by $\frac{1}{\sqrt{2}}$.

$$\text{Retarded peak uncertainty} = \sqrt{\frac{(7.5 \text{ keV})^2 + (3.0 \text{ keV})^2}{2}}$$

$$= \frac{1}{\sqrt{2}} \sqrt{(7.5 \text{ keV})^2 + (3.0 \text{ keV})^2}$$

so that $\Delta(\Delta E) = \sqrt{\frac{(7.5 \text{ keV})^2 + (3.0 \text{ keV})^2}{2} + (7.5 \text{ keV})^2 + (.012\Delta E)^2}$

or $\Delta(\Delta E) = \sqrt{89 \text{ (keV)}^2 + (.012\Delta E)^2}$

and $\frac{\Delta(\Delta E)}{\Delta E} = \sqrt{\frac{89 \text{ (keV)}^2}{(\Delta E)^2} + (.012)^2}$

(*) $\frac{\Delta(\Delta E)}{\Delta E} = \sqrt{\frac{89 \text{ (keV)}^2}{(\Delta E)^2} + .000144}$

where in all equations, ΔE is in keV.

Now $\frac{\Delta S}{S} = \sqrt{(.01)^2 + (.01)^2 + \left(\frac{\Delta(\Delta E)}{\Delta E}\right)^2}$, for Mu Metal foil

$\frac{\Delta S}{S} = \sqrt{(.01)^2 + (.005)^2 + \left(\frac{\Delta(\Delta E)}{\Delta E}\right)^2}$, for other targets

where $\frac{\Delta(\Delta E)}{\Delta E}$ is evaluated from equation (*).

The uncertainty in the energies at which the stopping powers are determined is more easily evaluated. The energy loss suffered by an alpha particle escaping from the middle of the americium source was calculated to be 59 keV. If a 14% uncertainty is assigned to this value, owing to inadequately precise knowledge of the areal density for the ^{241}Am source (Povelites, 1973), then the energy of such an alpha particle is $5.427 \pm .008$ MeV. For a given stopping power measurement then, the uncertainty in the energy E_1 at which the measurement is made is tentatively

$$\Delta E_1 = \sqrt{(8.0 \text{ keV})^2 + \left(\frac{\Delta(\Delta E)}{2}\right)^2}$$

where $E_1 \cong E_0 - \frac{\Delta E}{2}$

The energy correction factor to the stopping power curve described in the deuteron error analysis was also applied here in the cases where the total energy loss was large, say larger than 20% of the total alpha energy. For the same reason as given in the deuteron error analysis, an uncertainty of 10% was assigned to this correction factor. Then finally,

$$\Delta E_1 = \sqrt{(8.0 \text{ keV})^2 + \left(\frac{\Delta(\Delta E)}{2}\right)^2 + (0.1 \times \text{correction factor})^2}$$

where ΔE_1, ΔE, and the correction factor energy are in keV.

CHAPTER VI

RESULTS AND CONCLUSIONS

The objectives of these experiments were stated in the Introduction of this paper. Having measured the stopping powers, as given in Tables 3 and 6, the purely informational objective was attained. Two topics of interest remain to be discussed: comparison of results with Bragg's rule and with the predicted projectile z^3 effect.

In tests of Bragg's rule for the additivity of stopping effects in composite materials, the test parameter used herein was the mean excitation energy I. Bragg's rule states that

$$(**) \qquad \ln I_B = \sum_{i=1}^{n} a_i \ln I_i$$

where a_i = fraction of total electron population contributed by the i^{th} element of the composite material.

I_i = mean excitation energy of i^{th} element, and the sum extends over the number of elements in the composite material.

The goal here is to arrive at experimental I values for the composite materials involved and to compare these with their respective values I_B as predicted by Bragg's rule.

The stopping powers listed in Tables 3 and 6 for the various composite materials were fitted with the Bichsel energy loss computer code to extract experimental mean excitation energies. The function of the program is to calculate stopping powers for each of the composites

at the prescribed energies E_1 and for trial input values of the mean excitation energy I. The experimental value of I for a composite is that value which yields the least deviation of the calculated stopping powers (based on the Bethe-Bloch formula) from the experimental stopping power values. To elaborate, the program contains an error function $\sigma(I)$ defined by

$$\sigma(I) = \left[\frac{1}{N} \sum_{i=1}^{N} \left(\frac{S_e(E_{1i}) - S_c(E_{1i,i})}{\Delta S(E_{1i})} \right)^2 \right]^{\frac{1}{2}}$$

where $S_e(E_{1i})$ = experimental stopping power at energy E_{1i}

$\Delta S_e(E_{1i})$ = uncertainty in $S_e(E_{1i})$

$S_c(E_{1i}, I)$ = calculated stopping power at energy E_{1i} and for mean excitation energy I

and the sum extends over the number of energies N at which measurements were made. The value of I is varied in the program and that value at which $\sigma(I)$ reaches a minimum, call it $\bar{I}$, is then the best-fit experimental value of I.

In all cases here, $\sigma(\bar{I})$ was less than one. In fact, for composites with only single energy measurements, such as cases in the alpha particle experiment where only Havar stopping power was measured at more than one energy (i.e., two energies), $\sigma(\bar{I})$ must necessarily be zero. For every composite, the values of I for which $\sigma(I)$ remains less than unity are also acceptable as experimental values since they lie

within the accuracies of the experiments, about 2% in both experiments. The values of $\bar{I}$, I_B, $\sigma(\bar{I})$, and the range of acceptable I values, $\Delta \bar{I}$, and the relative deviation from Bragg's rule for each composite material are contained in Table 9.

The values, I_B, for the mean excitation energies for these composites as predicted by Bragg's rule were calculated from equation (**). These values are seen to depend on the values of I for the constituents of the composites. The I values for the constituents are experimentally based, and subject to some variation (around 5% for the lighter elements). This results in some arbitrariness in the values of I_B for the composites. Attempts were made to use the most recent published I values for the elements of the composites here. The values for these elements, along with the sources for such, are given in Table 10.

The experiments reveal the following:

1. Stopping powers of Havar and Mu Metal deviate only slightly from Bragg's rule. In both experiments, the ranges of the experimental values of I for these composites contain the theoretical Bragg values I_B. The result for Havar is in disagreement with the measurements of Porter *et al.* (1970), who found the experimental value of I for Havar to be about 250 eV, approximately 15% lower than I_B.
2. The experimental I value for Permalloy is 7.1% lower than the expected value I_B. This deviation is large enough to be significant. A fairly extensive search of the literature has revealed no other measurements for Permalloy.

TABLE 9

COMPARISON OF I_B WITH $\bar{I}$

Deuteron Experiment

Material	I_B (eV)	$\bar{I}$ (eV)	$\Delta\bar{I}$ (eV)	$\sigma(\bar{I})$	$\frac{I_B - \bar{I}}{I_B} \times 100$ (%)
Havar	295	301	288-313	.33	-2.4
Mu Metal	300	298	286-311	.12	+0.7
Permalloy	294	273	262-285	.37	+7.1

Alpha Particle Experiment

Havar	295	306	295-316	.35	-3.7
Mu Metal	300	294	283-306	0	+2.0
Mylar	74.2	84.8	79-91	0	-13.1
Teflon	108	121	114-128	0	-11.3

TABLE 10

MEAN EXCITATION ENERGIES

Element	I(ev)
Hydrogen (in compounds)	16.5[a]
Beryllium	64.2[b]
Carbon (in compounds)	78.5[a]
Carbon (in mixtures)	77.5[b]
Oxygen (in compounds)	96.0[a]
Fluorine	121.0[c]
Chromium	259.2[b]
Manganese	275.0[b]
Iron	282.1[b]
Cobalt	302.4[b]
Nickel	306.2[b]
Copper	319.0[b]
Molybdenum	433.9[c]
Tungsten	731.0[c]

[a] Fano, 1964, p. 311

[b] Bichsel, 1970, p. 78

[c] Turner, 1964, p. 100

3. The experimental value of I for Mylar is 13.1% greater than the expected value I_B, closely following a trend which has been noted for light solid composites in other experiments. Tschalar and Bichsel (1968) found that for Lucite ($C_5H_8O_2$), Sapphire (Al_2O_3), and Quartz (SiO_2), $\bar{I}$ exceeded I_B by 7.2%, 9.7% and 7.1% respectively. (The latter experimental I values are represented as accurate to within .5%). Mylar differs only slightly in chemical composition from Lucite, and if Tschalar's and Bichsel's constituent I values are used to calculate I_B, $\bar{I}$ for Mylar exceeds I_B by 11.0%. Experiments with alpha particles by De Croes et al. (1960) and by Fiedler and Ulrich (1967), although of limited experimental accuracy, show that for several organic materials, including Mylar, the experimental stopping power values were less than that expected applying Bragg's rule. This implies that $\bar{I}$ in each case exceeds I_B. In the paper by De Croes et al., the stopping power difference in the case of Mylar was 2.8%, which corresponds to a difference in I_B and $\bar{I}$ of about 10.5%, in very close agreement with the findings here.
4. The $\bar{I}$ values for Teflon exceeds I_B by 11.3%. Teflon is also a light composite ($(C_2F_4)_n$), and in view of the discussion above this deviation is not unreasonable. No other measurements for Teflon have been found in a literature search.

The projectile z^3 effect formulation of Ashley et al. (1973 a), states that the stopping power S as given by the Bethe-Bloch formula should be modified to include the z^3 effect by

$$S_1(E) = S(E) + \frac{\Delta S}{S}(E) \cdot S(E)$$

where $\frac{\Delta S}{S}(E)$ is the fractional change in the stopping power as given by the Bethe-Bloch formula at energy E, and

$$\frac{\Delta S}{S} = \frac{z}{Z^{\frac{1}{2}} x^{3/2}} \cdot \frac{F(b/x^{\frac{1}{2}})}{L(x)}$$

$$x = \frac{40.2\ E \quad (\text{in MeV})}{Z \cdot A \ (\text{in amu})}$$

E = energy of incident particle

Z = target atomic number

A = target atomic mass

z = projectile atomic number (charge)

b = 1.8, a nearly constant parameter

The functions $F(b/x^{\frac{1}{2}})$ and L (x) are rather complicated and have been tabulated by Ashley *et al.* (1973 b) for a wide range of arguments.

The above discussion holds for an elemental absorber. For a composite, the formula is similar,

$$\frac{\Delta S}{S} = \frac{z}{(40.2\ E/A)} \cdot \frac{\sum_i n_i Z_i^{3/2} \cdot \frac{F(b/\sqrt{x_i})}{\sqrt{x_i}}}{\sum_i n_i \cdot Z_i L(x_i)}$$

where the sum extends over the number of elements in the composite and n_i is the atomic concentration of element i.

Since $F(b/x^{\frac{1}{2}})$ and L (x) had been tabulated, this formulation was easily incorporated into the Bichsel code so that values of S_1 (E) could be determined for the composites used here. Inclusion of this projectile

z^3 effect significantly alters the best fit I values for Permalloy, Mu Metal, and Havar, as Table 11 indicates. For Havar and Mu Metal, the $\bar{I}$ values considerably exceed their respective I_B values. For Permalloy in the deuteron experiment, $\bar{I}$ exceeds I_B by only 2.7%. The previously excellent agreement with Bragg's rule for Havar and Mu Metal disappears with inclusion of this z^3 effect.

No data was fitted for Mylar and Teflon with inclusion of the z^3 effect. A recent study of stopping powers of hydrocarbon compounds has yielded results of doubtful validity when the z^3 effect formulation is included in fitting the data for the mean excitation energies. Atomic model inadequacies are believed to arise when the z^3 effect formulation is applied to targets of low average atomic number, say $Z < 13$ (Porter and Shepard, 1974).

The significance of the Havar, Mu Metal, and Permalloy results with the inclusion of the z^3 effect will now be explored. Inner shell corrections in the Bethe - Bloch formula were arrived at through fits of stopping power data (see Introduction). As pointed out by Ashley (1973), it may be that these shell corrections have incorporated within them the z^3 effect contribution to stopping power. If this is the case, then it is necessary to separate the z^3 effect from the shell corrections by some method in order to incorporate properly the z^3 effect. The technique requires many precise data points. Hence, the shell corrections were left fixed in the modified Bichsel code when the above data was fitted.

At low velocities, both the shell corrections and the z^3 effect

TABLE 11

COMPARISON OF I_B WITH $\bar{I}$ WITH
PROJECTILE z^3 EFFECT INCLUDED

Deuteron Experiment

Material	I_B (eV)	$\bar{I}$ (eV)	$G(I)$	$\frac{I_B - \bar{I}}{I_B} \times 100$ (%)
Havar	295	330	.10	-11.8
Mu Metal	300	327	.51	-9.0
Permalloy	293	301	.75	-2.7

Alpha Particle Experiment

Havar	295	358	.10	-21.4
Mu Metal	300	351	0	-17.0

correction become important. Bichsel, as stated previously, scaled the L-shell correction to get his experimental M-shell correction. The data which he used was taken over a wide energy range and hence the scaling parameters and perhaps the assumed shape of the M-shell correction very likely have incorporated the z^3 effect within them, or at least part of the z^3 effect. (Part of the z^3 correction may also be absorbed in the derived I value).

Then in fitting with the z^3 effect, with the shell corrections fixed, an additional term is added to the stopping power formula which has already been compensated for elsewhere. This leads to the enlargement of I values of Havar and Mu Metal produced by z^3 effect inclusion.

In view of the above discussion, extraction of mean excitation energies by use of the unmodified Bichsel code suffices for present purposes.

CHAPTER VII

SUMMARY

Two independent experiments were performed to determine stopping powers of several materials. Stopping powers were determined for Havar, Mu Metal, and Permalloy in the first experiment, which utilized deuterons. In the second experiment, which used alpha particles, stopping powers were determined for Havar, Mu Metal, Teflon, and Mylar. The results in both experiments show that Havar and Mu Metal obey Bragg's rule very closely. The result for Havar is in disagreement with measurements made by Porter et al. (1970). The Permalloy measurement with deuterons is in disagreement with Bragg's rule, with $\bar{I}$ 7.1% lower than I_B. The Teflon and Mylar measurements also show deviations from Bragg's rule, as has been observed in other recent experiments on similar light compounds. Reasons for these deviations are not fully known.

Tests of the z^3 effect formulation of Ashley et al. (1972) were inconclusive due both to experimental imprecision and inability to adequately incorporate input parameters and the z^3 effect formulation simultaneously within the Bichsel computer code. The divergence in the alpha particle stopping power of Havar and Mu Metal and deuteron stopping power of Havar and Mu Metal, predicted by the z^3 effect formulation because of the charge difference between alpha particles and deuterons, was not experimentally observable here because of the method used to

obtain the energy calibration curve for the alpha particle experiment. This curve was obtained by using the unmodified Bichsel computer code on aluminum and nickel data points. This version of the Bichsel computer code assumes a strict z^2 dependence of the stopping power formula on the charge of the incident particle. The deuteron and alpha particle stopping powers of Havar are graphed in Figure 8. This graph demonstrates the consistency of results between the alpha particle experiment and the deuteron experiment but cannot be used to extract information concerning the z^3 effect. Since the experiments described herein failed to provide information concerning the z^3 effect, this formulation is still in need of experimental investigation on materials of intermediate average atomic number.

FIGURE 8

STOPPING POWER CURVES OF HAVAR

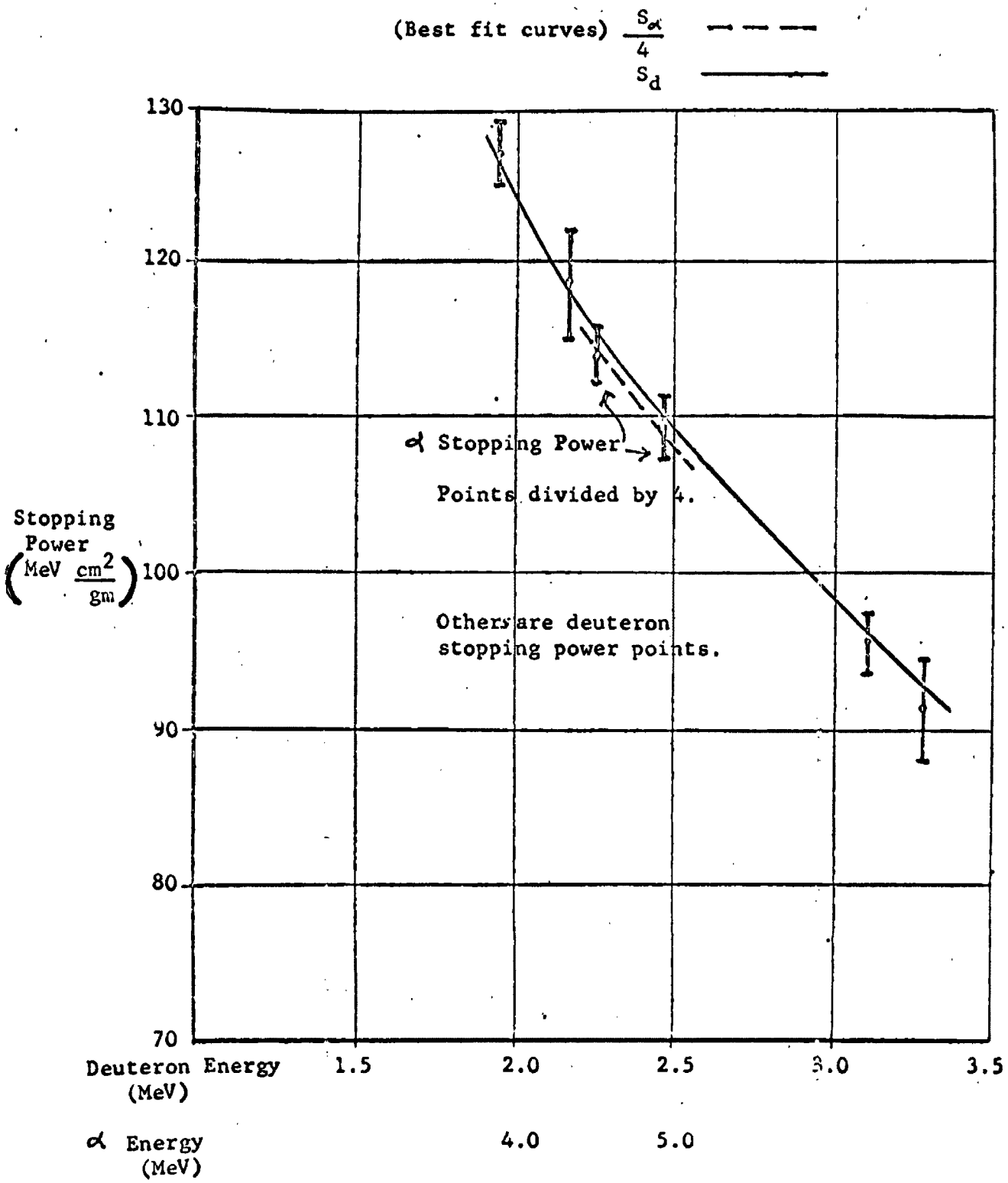

LIST OF REFERENCES

Ashley, J. (1973). Private communication. Preprint. "The Influence of the z^3 Contribution to Stopping Power on the Evaluation of Mean Excitation Potentials and Shell Corrections."

Ashley, J., Anderson, V., Ritchie, R., and Brandt, W. (1973b). Private communication. Preprint. "z^3 Effect in the Stopping Power of Matter for Charged Particles."

Ashley, J., Ritchie, R., and Brandt, W. (1972). "z^3 Effect in the Stopping Power of Matter for Charged Particles." Physical Review B, 5, 2393.

Ashley, J., Ritchie, R., and Brandt, W. (1973a). Private communication. Preprint. "On z^3 Dependent Stopping Power and Range Contributions."

Bichsel, H. (1967). "A FORTRAN Program for the Calculation of the Energy Loss of Heavy Charged Particles." University of California Lawrence Radiation Laboratory Report UCRL - 17538.

Bichsel, H. (1968). "Charged Particle Interactions." Radiation Dosimetry. ed. by F. Attix and W. Roesch. Academic Press, New York and London. Vol. I, Ch. 4, pp. 157-228.

Bichsel, H. (1970). "Passage of Charged Particles Through Matter." University of Southern California Report USC - 136-150.

De Croes, M., Parker, W., and Sevier, K. Jr. (1960). "Thin Film Thickness Distribution by Alpha Absorption." Nuclear Instruments and Methods. 7, 160.

Erginsoy, C., Wegner, H., and Gibson, W. (1964). "Anisotropic Energy Loss of Light Particles of MeV Energies in Thin Silicon Single Crystals." Physical Review Letters. 13, 530.

Fano, U. (1964). "Penetration of Protons, Alpha Particles, and Mesons." Studies in Penetration of Charged Particles in Matter. National Academy of Science - National Research Council Publication 1133, Washington D.C. pp. 287-352.

Fiedler, O., and Ulrich, O. (1967). "The Relative Stopping Power of Some Substances for Alpha Particles up to 5 MeV." Zie Physik. 200, 493. (Also, Oak Ridge National Laboratory Translation ORNL -tr- 1861 by R. Gregg Mansfield).

Gursky, J. (1973). Private communication.

Henkel, R. (1973). Private communication.

Niiler, A. (1969). Private communication. University of California, Los Alamos Scientific Laboratory, Office Memo., 6/20/69: "Bichsel Range - Energy Loss Code."

Porter, L., McIntyre, L., and Haeberli, W. (1970). "Stopping Power of Havar for 2.5 to 7.0 MeV Deuterons." Nuclear Instruments and Methods. 89, 237.

Porter, L., and Shepard, C. (1974). In preparation.

Povelites, J. (1973). Private communication.

Tschalar, C., and Bichsel, H. (1968). "Mean Excitation Energies of Light Compounds." Physical Review. 175, 476.

Turner, J., (1964). "Values of I and I_{adj} Suggested by the Subcommittee." Studies in Penetration of Charged Particles in Matter. NAS-NRC Pub. 1133, Washington D.C. pp. 99-101.

Walske, M. (1952). "The Stopping Power of K-Electrons." Physical Review. 88, 1283.

Walske, M. (1956). "The Stopping Power of L-Electrons." Physical Review. 101, 940.